# Nonequilibrium and Rarefaction Effects in Hypersonic Multicomponent Viscous Shock Layers

**V.V. Riabov**[1]

## 1 Introduction

Planetary exploration programs [1] stimulate new studies in hypersonic aerothermodynamics. The design of hypersonic vehicles has brought renewed interests in the heat protecting methods [2], [3], [4]. To analyze the structure of nonequilibrium airflow near a blunt body, a model of a thin viscous shock layer (TVSL) (an approximation of the Navier-Stokes equations) was developed [5]-[12].

In this paper, the streamlining of bodies of spherical and cylindrical shapes is studied using the TVSL model [8]-[12] with the generalized Rankine-Hugoniot relations [3], [8] under re-entry flight conditions at altitudes from 110 to 60 km. Various models of diffusion fluxes, surface catalysis, and chemical-reaction rates are studied. The catalytically influenced zone of the flow near the surface is analyzed. It is shown that body and shock slip models [13]-[15] are required with VSL calculations to receive physically meaningful results at high altitudes. TVSL results are compared with experimental data, solutions of the Navier-Stokes equations [16] and the Direct Simulation Monte Carlo (DSMC) technique [4], [17].

## 2 Approximation of a Thin Viscous Shock Layer (TVSL)

The boundary-value problem for the TVSL model was formulated in [5]-[12]. The TVSL equations are found from asymptotic analysis of the Navier-Stokes equations at $\varepsilon \to 0$, $Re_{of} \to \infty$, and $\delta = (\varepsilon Re_{of}) = \text{const}$, where $Re_{of} = \rho_\infty U_\infty R/\mu(T_{of})$ is Reynolds number, $\varepsilon = (\gamma\text{-}1)/(2\gamma)$, $\gamma$ is a specific heat ratio, and $T_{of}$ is stagnation temperature estimated at "frozen" upstream conditions [8]. For nonequilibrium flows, the TVSL equations were formulated in [3], [9]. Formulas for total enthalpy $H$, heat flux $q$, mass fluxes of species, specific heats, and species rates can be found

[1] *Rivier University, 420 S. Main St., Nashua, New Hampshire 03060, USA*

in [3], [10]. The method of calculating transport coefficients of dissociating gases is described in [18]. The conditions of adhesion and nonpenetration are specified at the body surface, as are the conditions of equilibrium-radiation heat exchange and mass component balances including surface catalysis. The generalized Rankine-Hugoniot conditions [3], [9], [10] are imposed at the TVSL external boundary.

## 3 Numerical Method and Validation of Computational Results

The numerical procedure developed in [9]-[12] was used for solving the TVSL equations using Keller's two-point second-order scheme [10]. Calculations were made in the whole range of chemical reaction rates up to the equilibrium values. The iteration process demonstrates a rapid convergence of the second order towards the solution. This property of the numerical algorithm is important when the influence of recombination processes on the flow structure is essential.

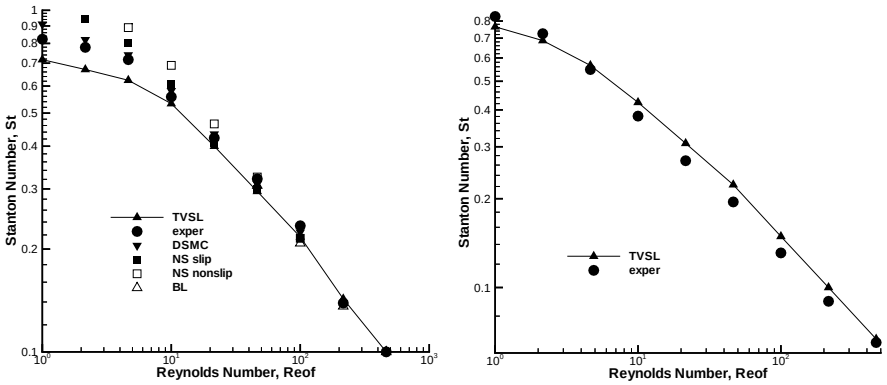


**Fig. 1** Stanton numbers *St* vs. Reynolds numbers $Re_{\mathrm{of}}$ for different medium models and various wind-tunnel experimental conditions [19], [20], [21] for a sphere (*left*) and a cylinder (*right*)

The Stanton numbers *St* at the stagnation point of a sphere were calculated under wind-tunnel conditions at various $Re_{\mathrm{of}}$, Mach number $M_\infty = 15$, and temperature factor $t_{\mathrm{w}} = 0.15$. The comparison between TVSL results (triangles) and solutions of the Navier-Stokes equations with slip (filled squares) and non-slip (empty squares) boundary conditions is shown in Fig. 1 (*left*). The results correlate well with experimental data [19]-[21] (circles) and DSMC data [4] (gradients). The TVSL results (triangles) for a cylinder also correlate well with experimental data [19] (circles) (see Fig. 1, *right*). A comparison between the TVSL results, experimental data [22] and DSMC data [4] along the spherical surface is shown in Fig. 2 (*left*).

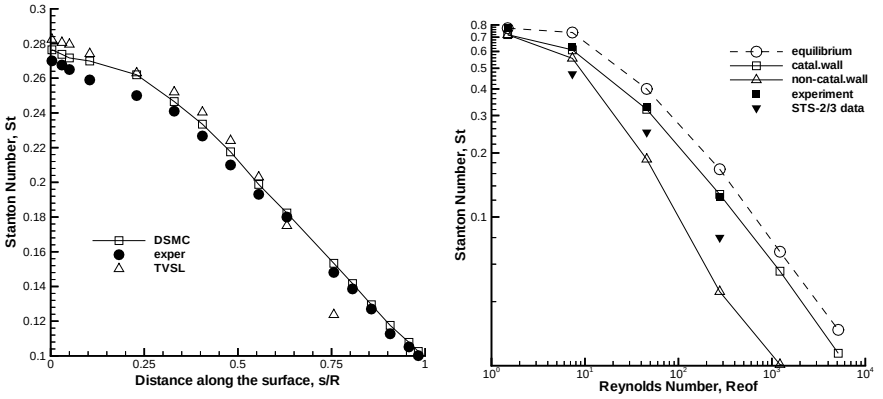


**Fig. 2** *Left*: Stanton numbers *St* along the spherical surface coordinate *s*/*R* at $Re_{\infty f}$ = 46.38, $M_\infty$ = 6.5, $t_w$ = 0.31, $\gamma$ = 1.4. *Right*: Stanton numbers *St* vs. Reynolds numbers $Re_{\infty f}$ for a sphere of radius *R* = 1 m along the Space Shuttle trajectory and different medium models

## 4 Computational Results for the Flight Conditions

Calculations were carried out for descent flight conditions of a blunt body in the Earth atmosphere at altitudes *h* = 110, 100, 90, 80, 70, and 60 km and Reynolds numbers $Re_{\infty f}$ = 1.49, 6.97, 47.3, 230, 1220, and 5130 per 1 m, correspondingly. The values of the Stanton number $St = q/(\rho_\infty U_\infty (H_0\text{-}H_w))$ in the critical point of a sphere (*R* = 1 m) along the Space Shuttle trajectory [23] are shown in Fig. 2 (*right*).

The surface catalysis significantly influences heat flux *q*. The values of *q* under the flight conditions at 80 km ($Re_{\infty f}$ = 230, $U_\infty$ = 7.9 km/sec) differ by factor of three for various catalytic surfaces due to the nonequilibrium character of physical and chemical processes in the VSL. This fact is confirmed by the STS-2/3 flight data [24] (filled triangles, Fig. 2, *right*). At the altitude *h* = 67.5 km this difference reaches 240 percent. The effect is less pronounced for catalytic surfaces [11]. The nonequilibrium TVSL results near catalytic surfaces correlate with the data (circles) [10] obtained for equilibrium VSL (see Fig. 2, *right*).

The catalysis does not noticeably influence pressure, VSL thickness, and coefficient of friction at $1.49 \le Re_{\infty f} \le 5130$. The calculated values of heat flux and species distributions for flight conditions at *h* = 60 - 110 km are displayed in Figs. 3, 4.

The degree of catalysis influences significantly distributions of mass concentrations $\alpha_i = \rho_i/\rho$ in the VSL (see Fig. 3, *left*). The measure of this influence is the width of the catalytically influenced zone *d*, which is characterized by the difference in distributions $\alpha_i$ for two extreme cases: ideally catalytic and absolutely non-catalytic surfaces. The flight conditions fully define the degree of dissociation of $O_2$, NO, $N_2$, concentrations of O and N atoms, and the size of the zone *d*.

The calculations of $\alpha_i$ on the external boundary of the TVSL at $1.49 \le Re_{\infty f} \le 5130$ indicate that the catalysis influences the full width of the VSL at altitudes

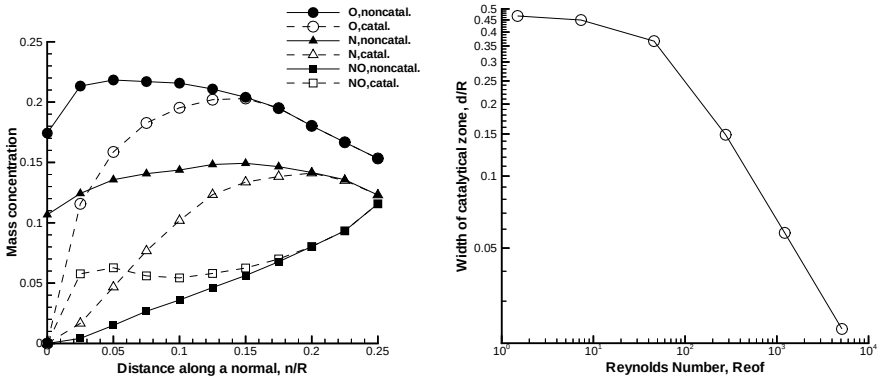


**Fig. 3** *Left*: Mass concentrations $\alpha_i$ of air components in the TVSL at $Re_{of}$ = 230. *Right*: The width of the catalytically influenced zone $d$ vs. Reynolds number $Re_{of}$

above 85 km. At the lower altitudes, species concentrations on the external boundary of the layer reach their values in upstream equilibrium flow [10], [11]. It is found that under the flight conditions at $h$ = 60 km, instead of the generalized Rankine-Hugoniot relations, it is possible to use standard boundary conditions [7] at the shock wave. The estimated values $d$ are shown in Fig. 3 (*right*).

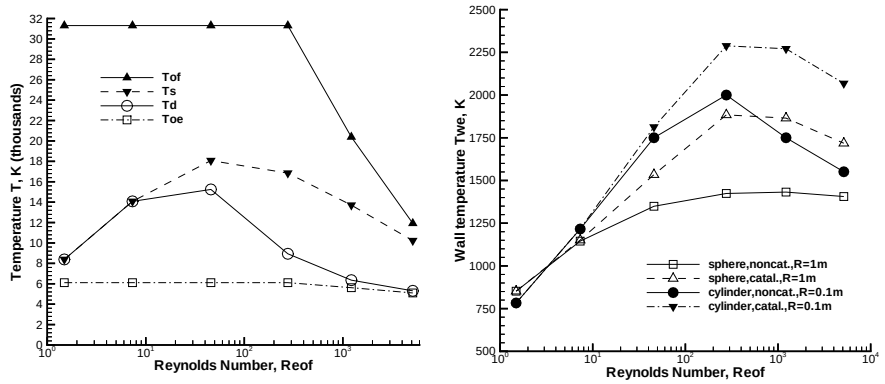


**Fig. 4** *Left*: The values of temperatures $T_s$, $T_d$, $T_{of}$, and $T_{oe}$ vs. Reynolds number $Re_{of}$. *Right*: Equilibrium temperature $T_{we}$ of spherical ($R$ = 1 m) and cylindrical ($R$ = 0.1 m) surfaces

Temperature values $T_s$ at the external boundary of TVSL (gradients), stagnation temperature $T_{of}$ (triangles), and values $T_d$ (circles) on the catalytically-influenced-zone boundary $d$ are shown in Fig. 4 (*left*). At $h \leq 90$ km, a decrease of $T_d$ is observed and its values merge with the temperature $T_{oe}$ (squares) estimated at the

equilibrium dissociated-air state behind the shock wave. As $Re_{of}$ increases, $T_s$ rises at h from 110 to 90 km. As the altitude falls below 80 km, due to the vehicle deceleration [23], a monotonous decrease of $T_s$ and $T_{of}$ is observed.

## 5 Equilibrium Temperature of the Vehicle Surface

Large values of the heat flux towards the body surface lead to high level of equilibrium surface temperature $T_{we} = (q/\varepsilon\sigma)^{1/4}$, where $\varepsilon$ is emissivity, and $\sigma$ is the Stephan-Boltzmann's constant. The values $T_{we}$ with $\varepsilon = 0.85$ are shown in Fig. 4 (*right*), for the critical point of a sphere ($R = 1$ m) and on the critical line of a cylinder ($R = 0.1$ m) for two extreme cases of surface catalysis. Using noncatalytic materials (solid lines) leads to a significant decrease in $T_{we}$. The calculations also indicate that values $T_{we}$ on the cylindrical surface monotonously decrease as the swept angle increases and only slightly depends on the mechanism of catalysis [12], [25].

## 6 The Binary-Scaling Similitude Law

Numerical results [8] show that parameters in the TVSL are frozen at $Re_{of} < 20$; recombination processes are negligible, and the binary-scaling similitude law [8], $\rho_\infty R = const$, can be applied at $U_\infty = const$. Calculations performed for the critical streamline assuming $U_\infty = 7.8$ km/s, $\rho_\infty R = 5.35 \times 10^{-7}$ kg/$m^2$ ($Re_{of} = 7.33$), and nose radii $R = 1$ m and 0.005 m show that distributions of flow parameters for these cases correlate satisfactorily. The temperature and electron concentration $N_e$ profiles near a noncatalytic surface are shown in Figs. 5 (*left*) and (*right*), correspondingly.

## 7 Conclusion

The computational tests were conducted as a model problem for preliminary design of heat protection systems of hypersonic vehicles. The results validate the TVSL model for calculating nonequilibrium multicomponent gas flow near blunt bodies under low-density flight and wind-tunnel test conditions. The study of characteristics of the catalytically influenced zone can be used in developing approximation methods of predicting heat fluxes.

**Acknowledgments.** The author expresses gratitudes to V. P. Provotorov and V. N. Gusev for participation in developing concepts and numerical algorithms.

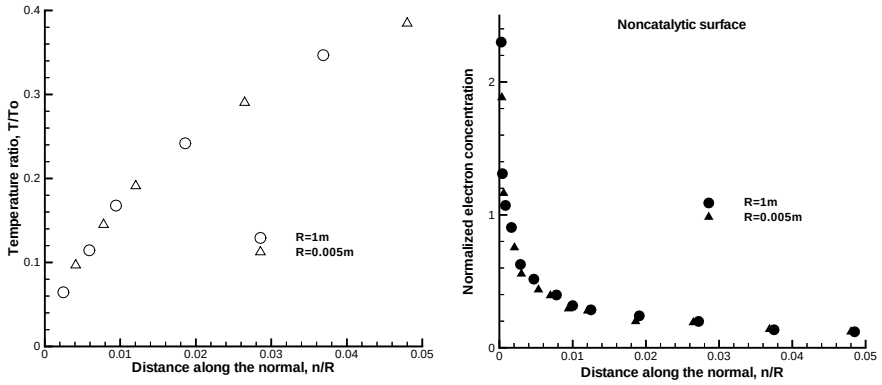


**Fig. 5** Temperature $T/T_o$ (*left*) and normalized electron concentration $N_e \times R \times 10^{-14}$ $m^{-2}$ (*right*) at the stagnation streamline of the sphere at $Re_{of}$ =7.33, $U_\infty$ = 7.8 km/s, $\rho_\infty R = 5.35 \times 10^{-7}$ kg/$m^2$

## References


1. Gnoffo, P.: Ann. Rev. Fluid Mech. **31**, 459-494 (1999)
2. Cheng, H.K.: Ann. Rev. Fluid Mech. **25**, 455-484 (1993)
3. Riabov, V.V., Botin, A.V.: J. Thermophys. Heat Transf. **9**(2) (1995)
4. Riabov, V.V.: J. Spacecr. Rockets **41**(4) (2004)
5. Cheng, H.K.: IAS Paper 63-92 (1963)
6. Moss, J.N.: NASA TR 411 (1974)
7. Miner, H., Lewis, C.: NASA CR 2550 (1975)
8. Gusev, V.N., Provotorov, V.P., Riabov, V.V.: Fluid Mech. - Sov. Res. **10**(5) (1981)
9. Provotorov, V.P., Riabov, V.V.: Trudy TsAGI **2111**, 142-156 (1981)
10. Provotorov, V.P., Riabov, V.V.: Fluid Mech. - Sov. Res. **12**(6) (1983)
11. Provotorov, V.P., Riabov, V.V.: Trudy TsAGI **2436**, 152-164 (1990)
12. Riabov, V.V., Provotorov, V.P.: AIAA Paper 94-2054 (1994)
13. Gupta, R., et al.: J. Spacecr. Rockets **27**(2) (1990)
14. Gupta, R., et al.: AIAA Paper 93-2724 (1993)
15. Gupta, R., Simmonds, A.: AIAA Paper 86-1349 (1986)
16. Molodtsov, V.K., Riabov, V.V.: Uch. Zap. TsAGI **10**(6) (1979)
17. Moss, J.N., Bird, G.A.: AIAA Paper 84-0223 (1984)
18. Riabov, V.V.: J. Thermophys. Heat Transf. **10**(2) (1996)
19. Botin, A.V., et al.: Trudy TsAGI **2436**, 134-144 (1990)
20. Nomura, S.: AIAA J. **22**(7) (1984)
21. Gusev, V.N., Nikolskiy, Yu.V.: Uch. Zap. TsAGI **2**(1) (1971)
22. Botin, A.V.: Uch. Zap. TsAGI **18**(5) (1987)
23. Tong, H., Buckingham, A., Curry, D.: AIAA Paper 74-518 (1974)
24. Throckmorton, D.: AIAA Paper 82-0003 (1982)
25. Gershbein, E., et al.: Fluid Dyn. **19**(6) (1984)